Spike Train Correlations Induced by Anatomical Microstructure

Stefan Rotter

Computational Neuroscience Lab
Bernstein Center Freiburg & Faculty of Biology
University of Freiburg, Germany

MathStatNeuro workshop • Laboratoire J. A. Dieudonné, Nice • September 8 – 10, 2015

stefan.rotter@biologie.uni-freiburg.de

Dynamic neuronal networks of the brain

Correlations and population signals

Disentangling multi-synaptic pathways

Inferring connectivity from correlations

Dynamic neuronal networks of the brain

Correlations and population signals

Disentangling multi-synaptic pathways

Inferring connectivity from correlations

Ramón y Cajal, 1900

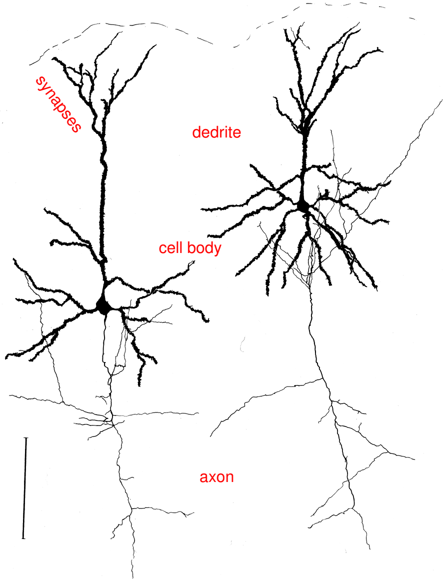

Braitenberg, 1978

The leaky integrate-and-fire model

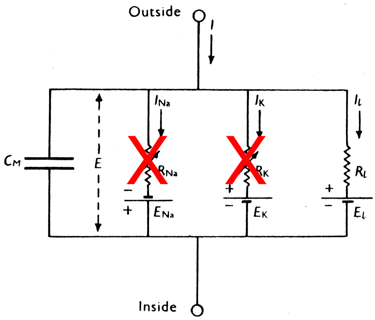

$$C\,\dot{U} + \frac{1}{R}\left[U - U_{\text{rest}}\right] = I$$

dynamical variables:	
$U(t)$	membrane potential
$I(t)$	input current
fixed parameters:	
C	membrane capacitance
R	membrane resistance
U_{rest}	resting potential
U_{thresh}	threshold potential

Simplifications implied by the leaky integrate-and-fire model:

point neuron	all parts of the neuron are iso-potential
linearity of integration	linear differential equation / linear system
time-invariance	parameters do not change in time

Current injection into neurons

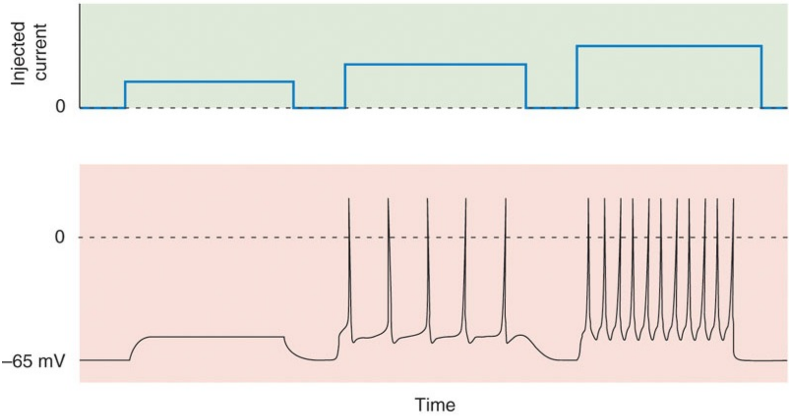

If injected current does not depolarize the membrane to threshold, no action potentials will be generated.

If injected current depolarizes the membrane beyond threshold, action potentials will be generated.

The action potential firing rate increases as the depolarizing current increases.

Chemical synapses

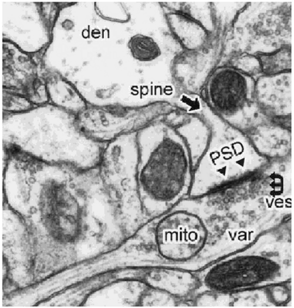

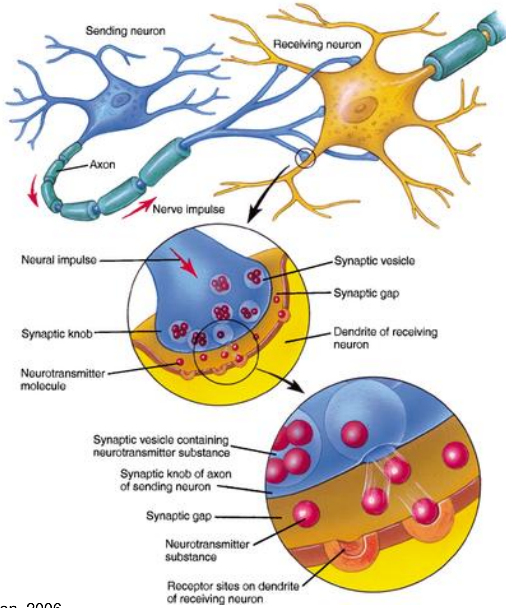

Source:
Mark Bear, Barry Connors, Michael Paradiso
Neuroscience: Exploring the Brain, Third Edition, 2006

Intracellular recording *in vivo*

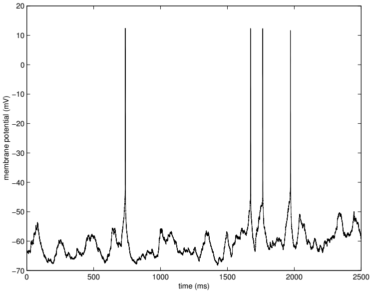

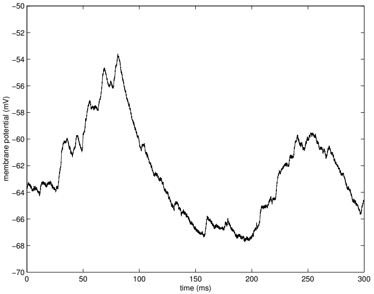

courtesy of V. Bringuier and Y. Fregnac

The leaky integrate-and-fire neuron model

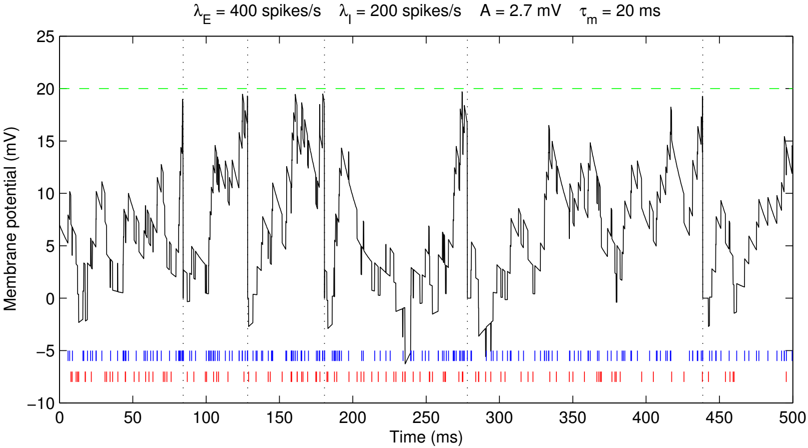

$$I(t) = \sum_k J_k \, \delta(t - t_k) \qquad \text{(here: } J_k = \pm A\text{)}$$

The Mouse Cortex

Total volume	$2\times87\,\mathrm{mm}^3$
Total number of neurons	16 000 000
Number of sensory input fibres	$<$ 1 000 000
Length of axonal tree	10–40 mm
Length of dendritic tree	4 mm
Range of axons	1/0.2 mm
Range of dendrites	0.2 mm
Density of neurons	90 000 /mm^3
Density of axons	4 km/mm^3
Density of dendrites	0.4 km/mm^3
Density of synapses	700 000 000 /mm^3
Synapses per neuron	8 000
Probability of synaptic contact	0.1
Relative density of axons	$10^{-5}/10^{-3}$
Relative density of dendrites	10^{-3}

Valentino Braitenberg & Almut Schüz
Cortex: Statistics and Geometry of Neuronal Connectivity
Second Edition, Berlin: Springer, 1998

Biological neuronal networks (BNN)

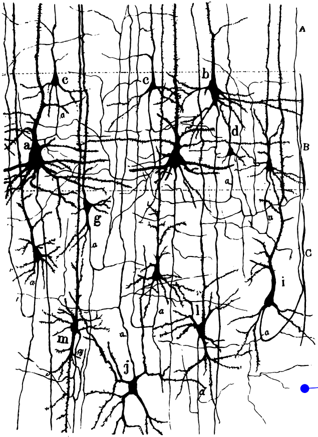

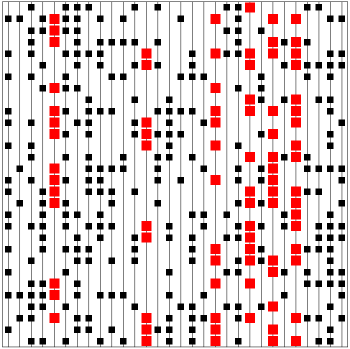

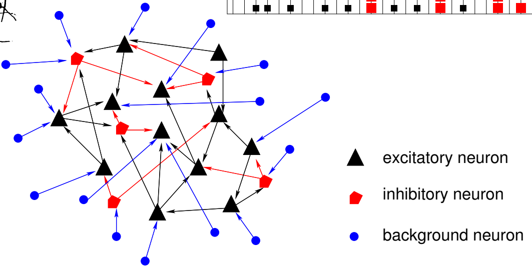

High-Performance Neuro-Computing (HPNC)

compute cluster *Hathor*

# processors/cores	$24 \times 2 \times 2 = 96$
RAM	24×8 GByte $= 192$ GByte
connectivity	high-speed Infiniband

nest::
simulated()

http://www.nest-initiative.org

Dynamic neuronal networks of the brain

Correlations and population signals

Disentangling multi-synaptic pathways

Inferring connectivity from correlations

Two different network topologies

Biological neurons

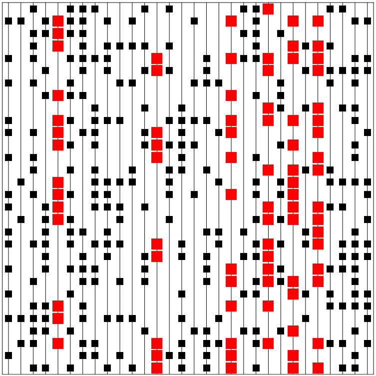

Hybrid neurons

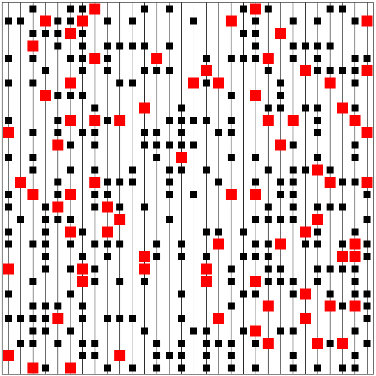

Mean input to individual neurons is identical in both cases!

Population fluctuations depend on correlations

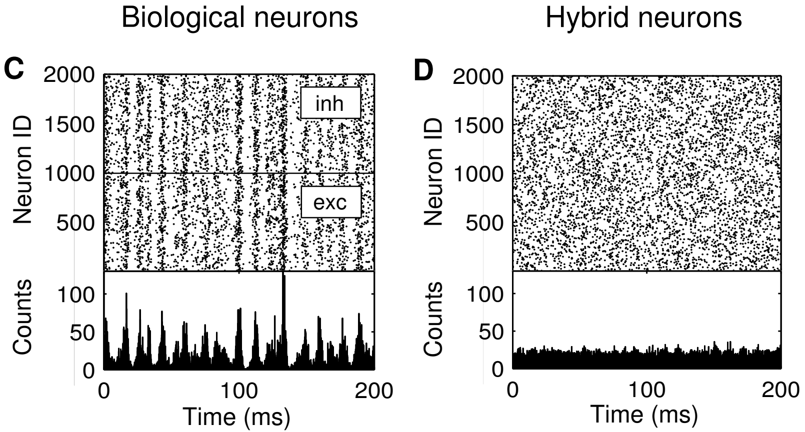

Kriener et al., *Neural Computation*, 2008

Population fluctuations depend on correlations

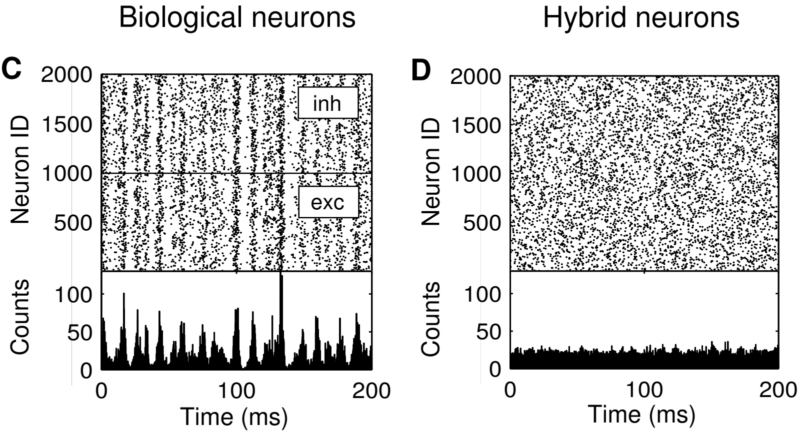

$$\mathbb{V}\mathrm{ar}\left[\sum_i X_i\right] = \sum_i \mathbb{V}\mathrm{ar}[X_i] + \sum_{i \neq j} \mathbb{C}\mathrm{ov}[X_i, X_j]$$

Kriener et al., *Neural Computation*, 2008

Shared input structure differs

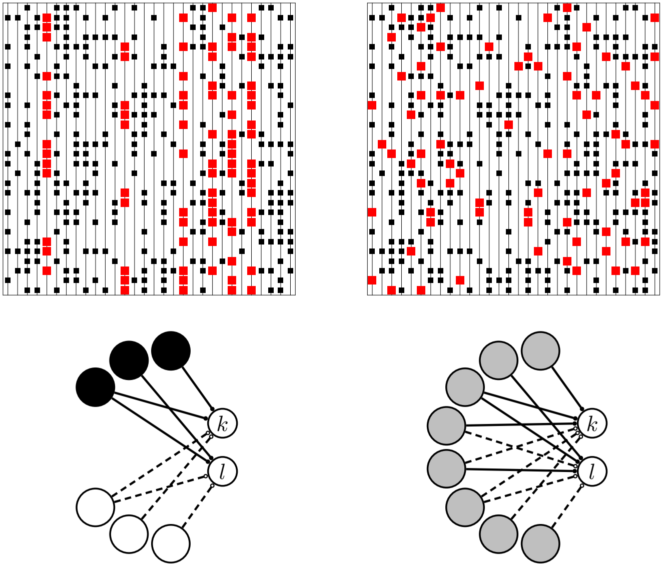

Recording from localized neuronal populations

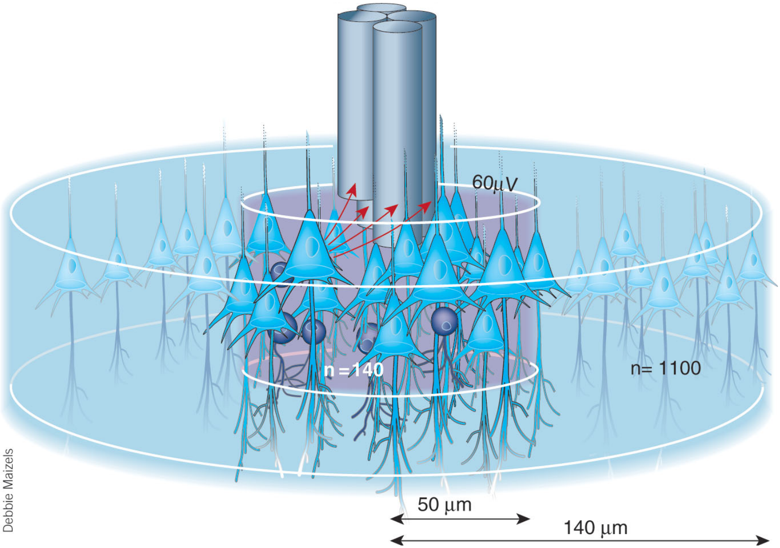

Buzsáki, *Nature Neuroscience*, 2004

Tuning of the LFP during arm movements

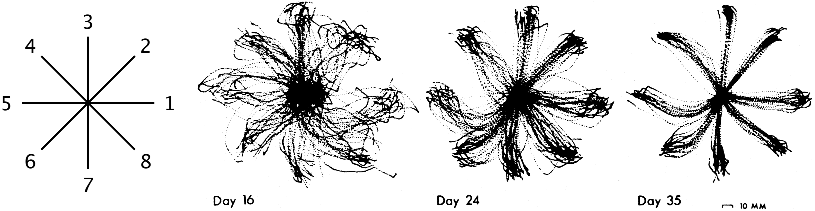

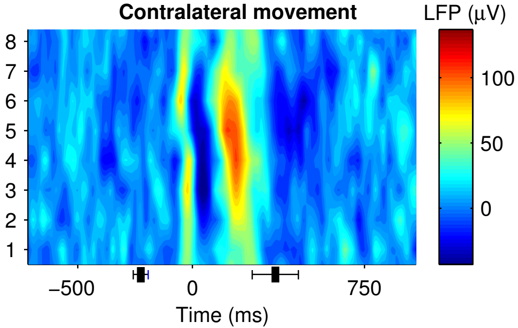

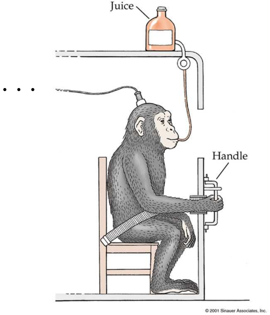

Mehring et al., *Nature Neuroscience*, 2003

Decoding of arm movements

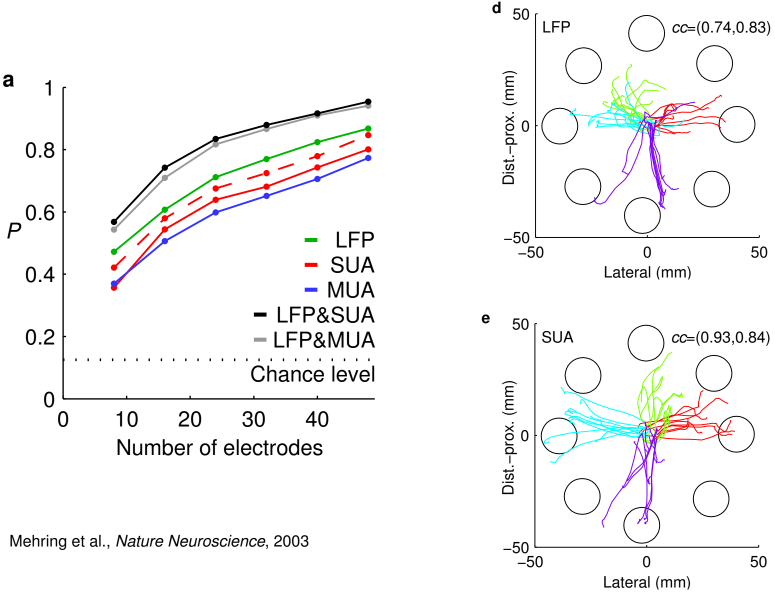

Mehring et al., *Nature Neuroscience*, 2003

Dynamic neuronal networks of the brain

Correlations and population signals

Disentangling multi-synaptic pathways

Inferring connectivity from correlations

Neuronal microcircuits

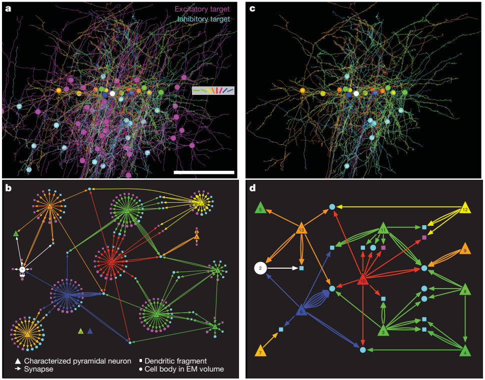

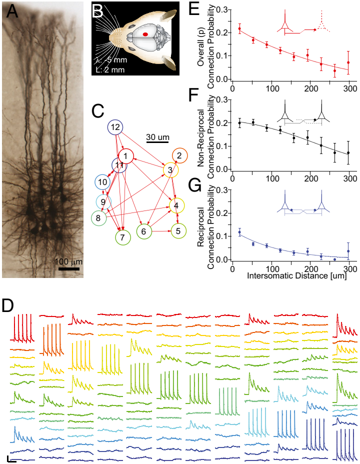

Mouse visual cortex
Calcium imaging *in vivo* + electron microscopy *in vitro*
Bock et al., *Nature*, 2011

Rat somatosensory cortex
12-fold patch recording *in vitro*
Perin et al., *PNAS*, 2011

How does connectivity induce correlations. . .

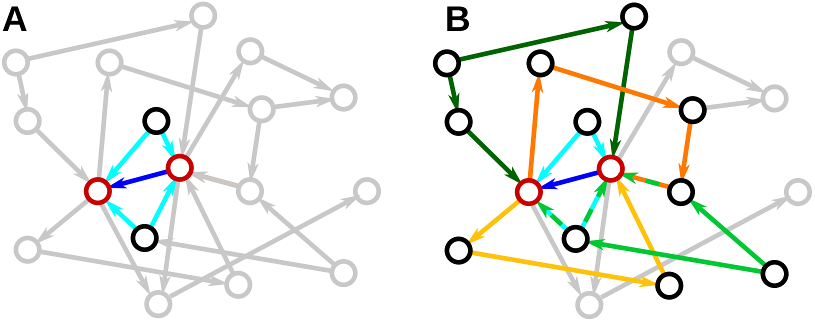

Pernice, Staude, Cardanobile, Rotter, *PLoS Computational Biology* 7(5): e1002059, 2011
Pernice, Staude, Cardanobile, Rotter, *Phys Rev E* 85: 031916, 2012
Pernice, Rotter, *Journal of Statistical Mechanics* P03008, 2013

Rangan, *PRL* 102(15): 158101, 2009; *PRE* 80(3): 036101, 2009
Trousdale, Hu, Shea-Brown, Josić, *PLoS Computational Biology* 8(3): e1002408, 2012

. . . and to which degree can
connectivity be inferred from correlations?

Undirected and directed graphs

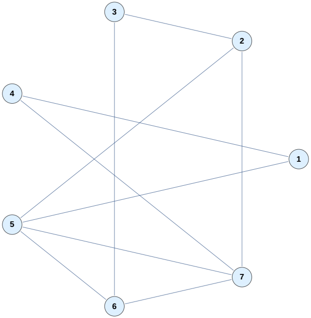

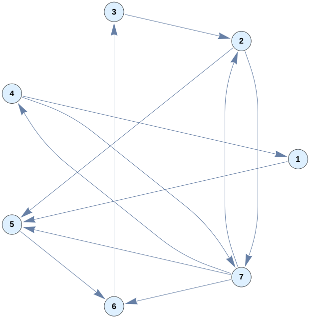

A graph consists of vertices (nodes) and edges (links). Each edge connects one pair of vertices. Connections can be either undirected (left) or directed (right).

The adjacency matrix of an undirected graph

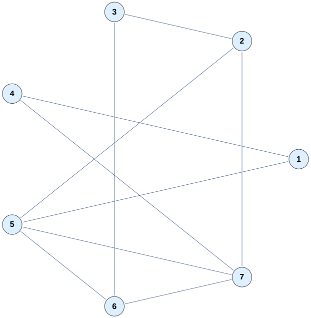

$$\begin{pmatrix} 0 & 0 & 0 & 1 & 1 & 0 & 0 \\ 0 & 0 & 1 & 0 & 1 & 0 & 1 \\ 0 & 1 & 0 & 0 & 0 & 1 & 0 \\ 1 & 0 & 0 & 0 & 0 & 0 & 1 \\ 1 & 1 & 0 & 0 & 0 & 1 & 1 \\ 0 & 0 & 1 & 0 & 1 & 0 & 1 \\ 0 & 1 & 0 & 1 & 1 & 1 & 0 \end{pmatrix}$$

The adjacency matrix $A = (a_{ij})$ fully describes the graph, provided that each vertex has been assigned a unique label. We have $a_{ij} = 1$ if vertex i and vertex j are connected, and $a_{ij} = 0$ otherwise. Because edges are undirected, the matrix is symmetric, i.e. $a_{ij} = a_{ji}$ for all i and j, and $A = A^T$.

The adjacency matrix of a directed graph

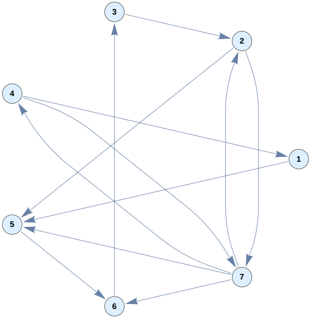

$$\begin{pmatrix} 0 & 0 & 0 & 1 & 0 & 0 & 0 \\ 0 & 0 & 1 & 0 & 0 & 0 & 1 \\ 0 & 0 & 0 & 0 & 0 & 1 & 0 \\ 0 & 0 & 0 & 0 & 0 & 0 & 1 \\ 1 & 1 & 0 & 0 & 0 & 0 & 1 \\ 0 & 0 & 0 & 0 & 1 & 0 & 1 \\ 0 & 1 & 0 & 1 & 0 & 0 & 0 \end{pmatrix}$$

Again, the adjacency matrix $A = (a_{ij})$ fully describes a graph with labeled vertices. We set $a_{ij} = 1$ if there is a link from j to i, and $a_{ij} = 0$ otherwise. Because here edges are directed, the matrix is asymmetric, i.e. $a_{ij} \neq a_{ji}$ and $A \neq A^T$. The transposed matrix A^T corresponds to a graph with all arrows reversed.

The in-degree and out-degree of a directed graph

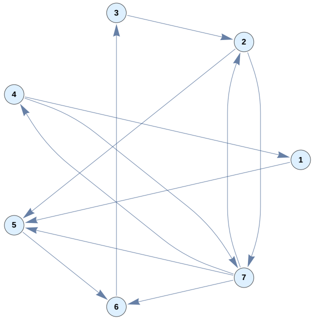

$$\begin{pmatrix} 0 & 0 & 0 & 1 & 0 & 0 & 0 \\ 0 & 0 & 1 & 0 & 0 & 0 & 1 \\ 0 & 0 & 0 & 0 & 0 & 1 & 0 \\ 0 & 0 & 0 & 0 & 0 & 0 & 1 \\ 1 & 1 & 0 & 0 & 0 & 0 & 1 \\ 0 & 0 & 0 & 0 & 1 & 0 & 1 \\ 0 & 1 & 0 & 1 & 0 & 0 & 0 \end{pmatrix}$$

The in-degree of a vertex is the number of its incoming edges, the number of its outgoing edges is called out-degree. In the adjacency matrix, the in-degree is the sum of all entries in the corresponding row. The out-degree is the sum of all entries in the corresponding column.

Graphs with weighted or multiple edges

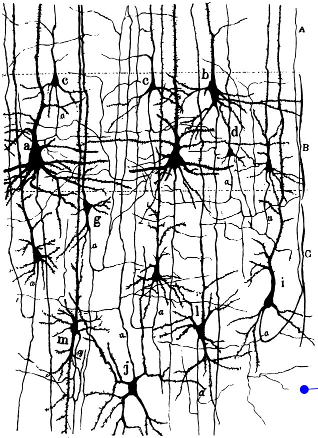

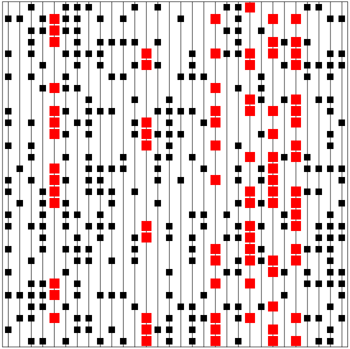

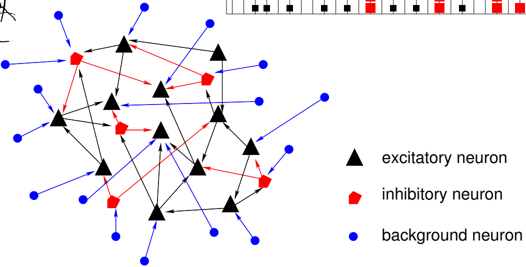

Paths in a graph

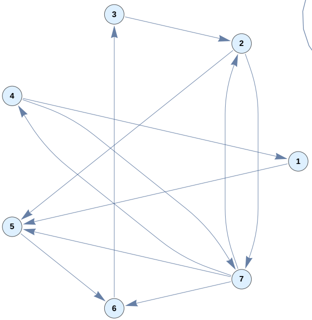

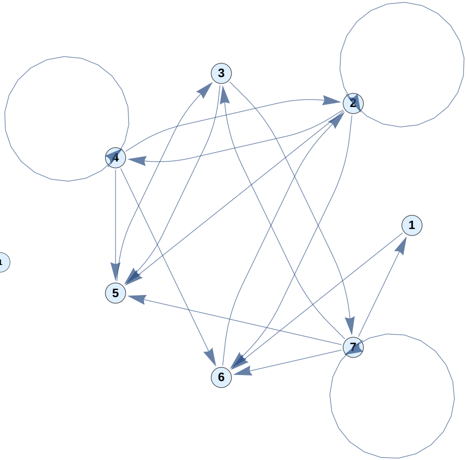

Starting from a given node, one can follow the links (if there are any) through the graph, respecting their orientation. If the out-degree of a vertex is larger than one, the path bifurcates. The graph that indicates which nodes can be reached after two hops can have multiple edges between any two vertices (not shown).

Powers of the adjacency matrix

$$\begin{pmatrix} 0 & 0 & 0 & 0 & 0 & 0 & 1 \\ 0 & 1 & 0 & 1 & 0 & 1 & 0 \\ 0 & 0 & 0 & 0 & 1 & 0 & 1 \\ 0 & 1 & 0 & 1 & 0 & 0 & 0 \\ 0 & 1 & 1 & 2 & 0 & 0 & 1 \\ 1 & 2 & 0 & 1 & 0 & 0 & 1 \\ 0 & 0 & 1 & 0 & 0 & 0 & 2 \end{pmatrix}$$

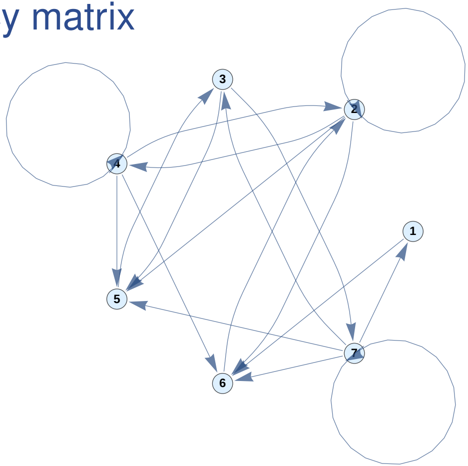

The graph that indicates which vertex can be reached after two hops corresponds to the square of the adjacency matrix A^2. Because this derived graph can have multiple edges between any two vertices, A^2 can have entries greater than one. Accordingly, the matrix power A^k corresponds to paths of length k.

The Hawkes process

A network of N nodes (neurons) is described in terms of

spike train	$s_i(t) = \sum_k \delta(t - t_k^i)$
firing rate	$y_i(t) = \langle s_i(t) \rangle$
external input	$y_0 \geq 0$
interaction kernel	$G(t) = \big(g_{ij}(t)\big)$

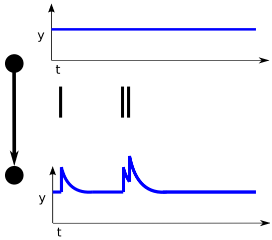

Its dynamics is defined in terms of the linear integral equation

$$y(t) = y_0 + \int_{-\infty}^{\infty} G(\tau) s(t - \tau)\, d\tau = y_0 + (G * s)(t).$$

Hawkes, 1971

Stationary firing rates

Assuming stationarity $y(t) = y$, one has

$$y = y_0 + \int_{-\infty}^{\infty} G(\tau) y \, d\tau = y_0 + Gy$$

with

$$G = \int_{-\infty}^{\infty} G(\tau) \, d\tau.$$

If the matrix $\mathbb{1} - G$ is invertible we have

$$y = [\mathbb{1} - G]^{-1} y_0.$$

If, in addition, $|\lambda| < 1$ for all eigenvalues λ of G, the usual geometric series expansion suggests a decomposition into contributions of recurrent pathways of all orders

$$y = [\mathbb{1} - G]^{-1} y_0 = \left[\sum_{n=0}^{\infty} G^n \right] y_0 = y_0 + G y_0 + G^2 y_0 + \ldots$$

Stationary correlations

Assuming joint stationarity, the pulse-coded interactions are conveniently quantified by the covariance functions

$$c_{ij}(\tau) = \mathbb{C}\text{ov}\big[s_i(t+\tau), s_j(t)\big] = \big\langle s_i(t)s_j(t+\tau)\big\rangle - \big\langle s_i(t)\big\rangle\big\langle s_j(t)\big\rangle.$$

Using Fourier transforms

$$\hat{f}(\omega) = \int_{-\infty}^{\infty} f(t)e^{-i\omega t}\,dt \qquad \text{and} \qquad \hat{f}(0) = \int_{-\infty}^{\infty} f(t)\,dt$$

Using Wiener-Hopf theory, Hawkes (1971) obtained for linearly interacting point processes

$$\big(\hat{c}_{ij}(\omega)\big) = \hat{C}(\omega) = \big[\mathbb{1} - \hat{G}(\omega)\big]^{-1} Y \big[\mathbb{1} - \hat{G}(\omega)^*\big]^{-1}$$

where $Y = \text{diag}(y)$. For the integrated covariances, one gets

$$C = \hat{C}(0) = \big[\mathbb{1} - G\big]^{-1} Y \big[\mathbb{1} - G^T\big]^{-1}.$$

Expanding correlations

Assuming again $|\lambda| < 1$ for all eigenvalues λ of G, the expansion of $[\mathbb{1} - G]^{-1}$ can be exploited to re-write the covariance ($Y = \mathbb{1}$)

$$C = [\mathbb{1} - G]^{-1}[\mathbb{1} - G^T]^{-1} = \Big[\sum_{n=0}^{\infty} G^n\Big]\Big[\sum_{m=0}^{\infty} \left(G^T\right)^m\Big]$$

$$= \ \mathbb{1} \ + \ G \ + \ G^T \ + \ G^2 \ + \ \left(G^T\right)^2 \ + \ GG^T \ + \ \ldots$$

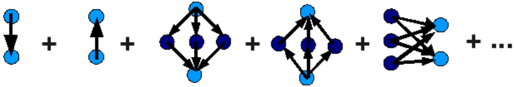

with matrix elements

$$g_{ij}^{(2,0)} \equiv \left(G^2\right)_{ij} = \sum_k g_{ik}g_{kj}, \quad g_{ij}^{(1,1)} \equiv \left(GG^T\right)_{ij} = \sum_k g_{ik}g_{jk}, \quad \ldots$$

corresponding to shared input contributed by different types of multi-synaptic pathways (motifs).

Pernice et al., 2011

Shared input motifs contributing to correlations

A

Matrix $G^{(n,m)}$	Elements $g_{ij}^{(n,m)}$	Symbol for $g^{(n,m)}$
GY	$g_{ij}y_{jj}$	
YG^T	$y_{ii}g_{ji}$	
G^2Y	$\sum_k g_{ik}g_{kj}y_{jj}$	
GYG^T	$\sum_k g_{ik}y_{kk}g_{jk}$	
$Y(G^T)^2$	$\sum_k y_{ii}g_{ki}g_{jk}$	
G^2YG^T	$\sum_{k_1,k_2} g_{ik_1}g_{k_1k_2}y_{k_2k_2}g_{jk_2}$	

B

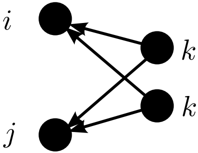

C

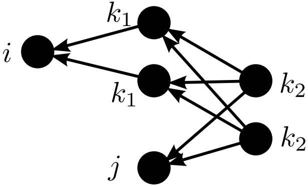

Fluctuations of population activity

Fluctuations of stationary population activity

$$S(t) = \sum_i s_i(t)$$

can be expanded into contributions from all auto- and cross-covariances

$$\mathbb{C}\mathrm{ov}\big[S(t+\tau), S(t)\big] = \sum_{ij} \mathbb{C}\mathrm{ov}\big[s_i(t+\tau), s_j(t)\big].$$

For a Hawkes process, we can exploit the power series expansion for the matrix of integrated covariances

$$\sum_{ij} C_{ij} = \sum_{ij} \sum_{nm} g_{ij}^{(n,m)} = \sum_{nm} \sum_{ij} g_{ij}^{(n,m)} = \sum_{nm} N^2 g^{(n,m)}.$$

Negative feedback decorrelates activity

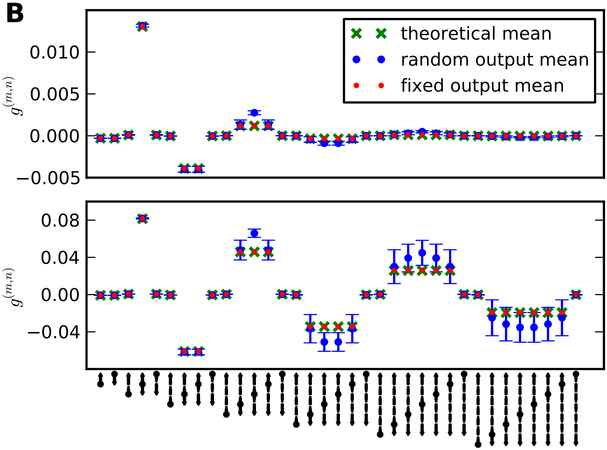

$p = 0.1$

$p = 0.25$

Average correlations in (almost) regular networks do not depend on fine-scale structure. For dominant recurrent inhibition, motifs of uneven order $m + n$ contribute negatively.

Non-regular networks: cliques of excitatory hubs

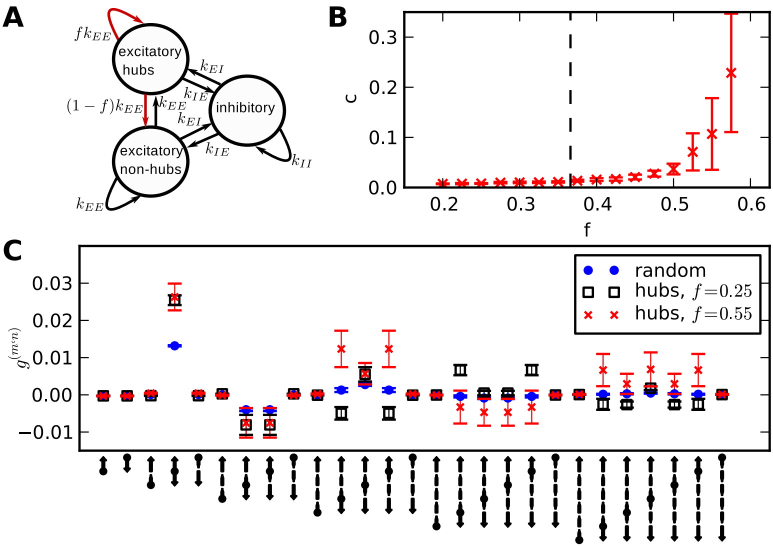

Patchy and/or cell-type specific connectivity

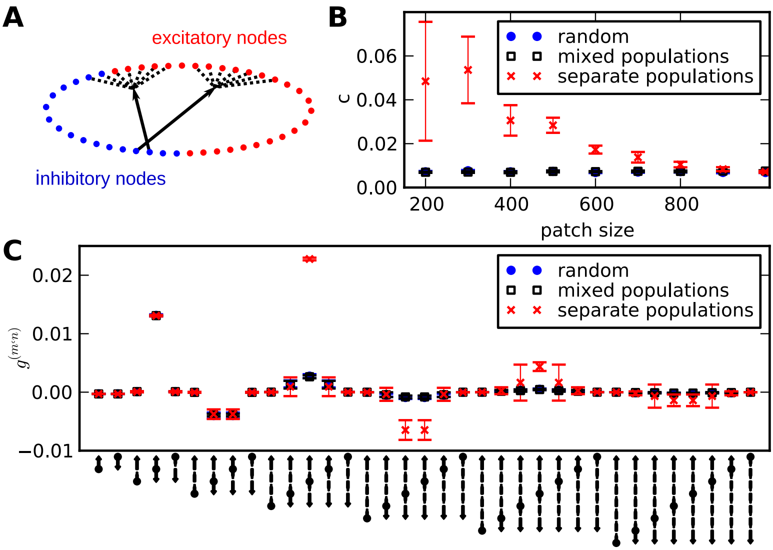

Correlations in networks of LIF neurons

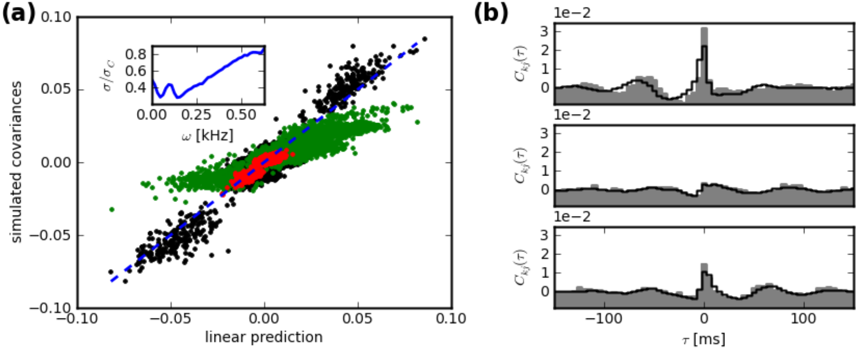

$\hat{c}_{ij}(\omega = 0)$

$\mathrm{Re}[\hat{c}_{ij}(\omega = 310\,\mathrm{Hz})]$

$\mathrm{Im}[\hat{c}_{ij}(\omega = 310\,\mathrm{Hz})]$

cross-correlation

Pernice et al., *Phys Rev E* 2012

Higher-order cumulants

Multivariate Hawkes process

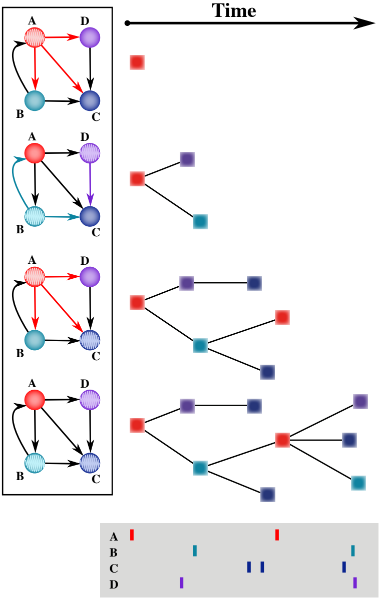

Hawkes, Oakes, *J Appl Prob*, 1974
Saichev, Sornette, *Phys Rev E*, 2014
Jovanović, Hertz, Rotter, *Phys Rev E*, 2015

A combinatorial challenge

$n = 2$

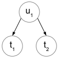

$n = 3$

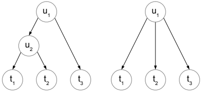

$n = 4$

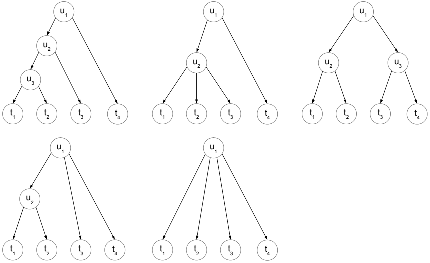

n	Terms in nth order density
2	1
3	4
4	26
5	236
6	2,752
7	39,208
8	660,302
9	12,818,912
10	282,137,824
11	6,939,897,856
12	188,666,182,784
13	5,617,349,020,544
14	181,790,703,209,728
15	6,353,726,042,486,272
16	238,513,970,965,257,728
17	9,571,020,586,419,012,608
18	408,837,905,660,444,010,496
19	18,522,305,410,364,986,906,624
20	887,094,711,304,119,347,388,416

Jovanović, Hertz, Rotter, *Phys Rev E*, 2015

Dynamic neuronal networks of the brain

Correlations and population signals

Disentangling multi-synaptic pathways

Inferring connectivity from correlations

Inferring directions from a symmetric matrix?

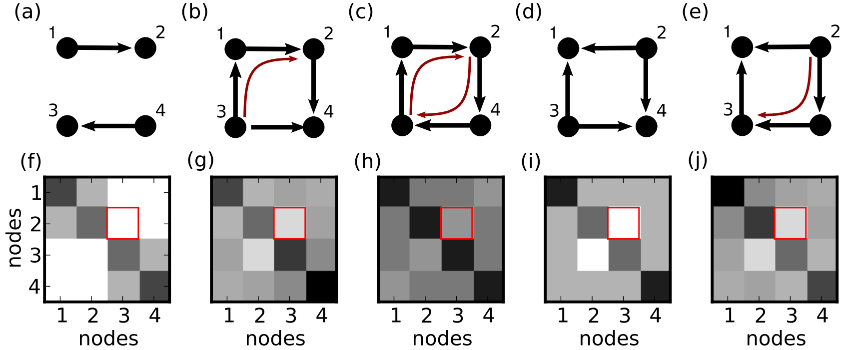

Pernice & Rotter, *JSTAT*, 2013

Fundamental degeneracy of the problem

Given the covariance matrix $\hat{C}(\omega)$, can one solve the equation

$$\hat{C}(\omega) = \big[\mathbb{1} - \hat{G}(\omega)\big]^{-1} Y \big[\mathbb{1} - \hat{G}(\omega)^*\,\big]^{-1}$$

for the connectivity matrix $\hat{G}(\omega)$? The Idea followed here is to determine “some” square root of the inverse covariance matrix

$$\hat{C}^{-1}(\omega) = \hat{B}(\omega)^*\,\hat{B}(\omega)$$

and extract $\hat{G}(\omega)$ from the relation (assuming Y is known)

$$\hat{B}(\omega) = Y^{-1/2}\big[\mathbb{1} - \hat{G}(\omega)\big].$$

However, for any unitary matrix U satisfying $U^*U = UU^* = \mathbb{1}$ the matrix $\hat{A} = U\hat{B}$ provides an equivalent solution

$$\hat{A}^*\,\hat{A} = \hat{B}^*\,U^*\,U\,\hat{B} = \hat{B}^*\,\hat{B}.$$

Searching for sparse networks

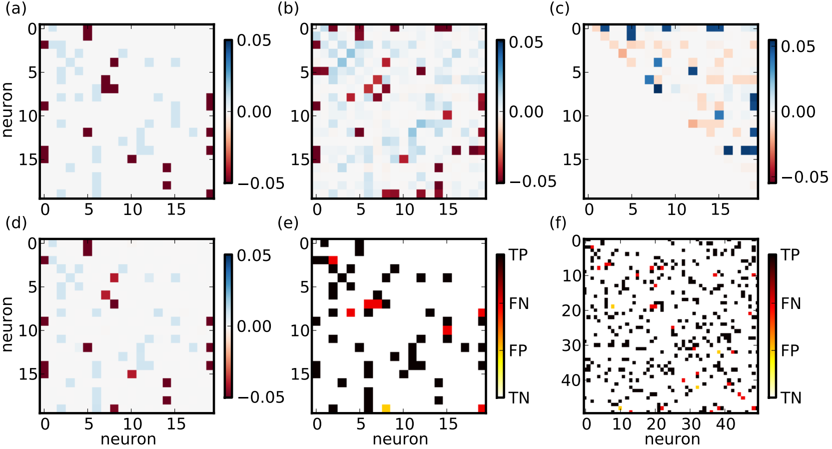

Method: stochastic minimization of the L_1-norm of the coupling matrix, using the Cholesky decomposition to initiate the search

Inference of connectivity from noise-free $\hat{C}(0)$

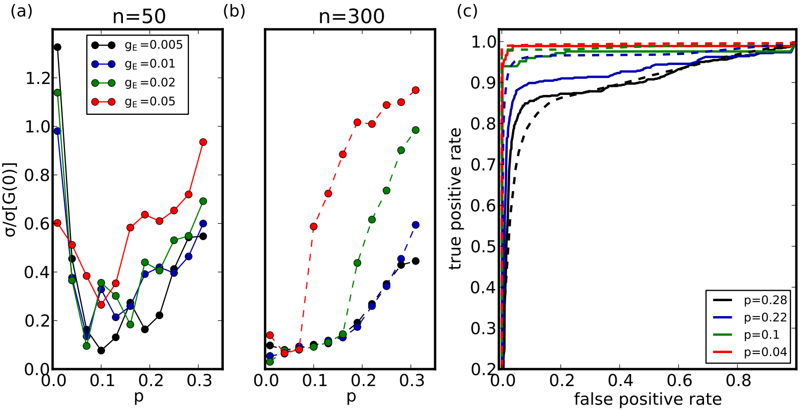

Inference of connectivity from estimated $\hat{C}(\omega)$

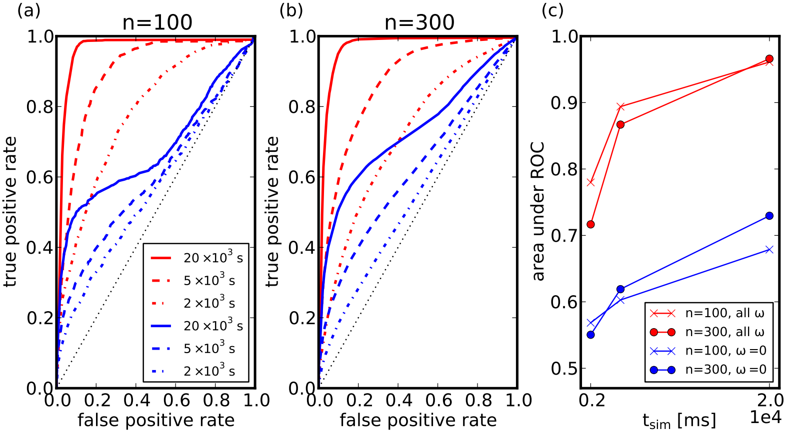

New applications: “networks of networks”

MUA	multi-unit activity
LFP	local field potentials
ECoG	electro-corticogram
MREG	MR-encephalography (“gradient-less imaging”)
NIRS	Near-infrared spectroscopy

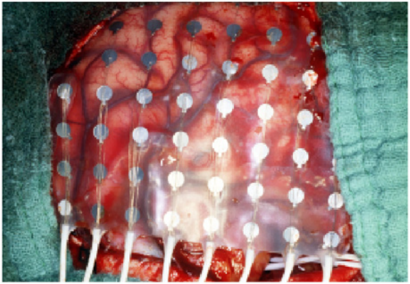

Pistohl et al., 2008 — 10 mm

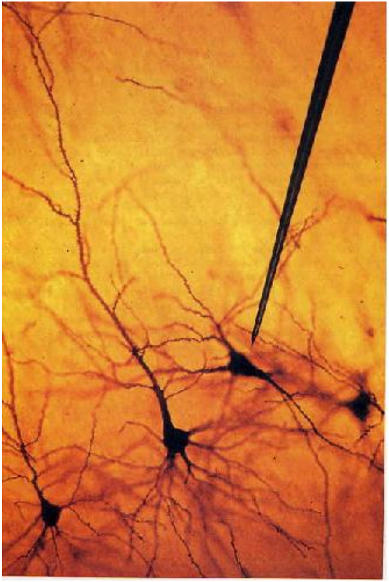

10 μm — Hubel, 1995

New applications: “networks of networks”

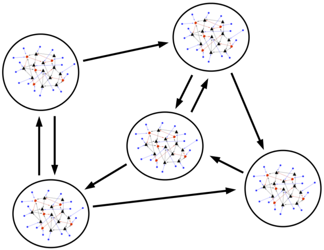

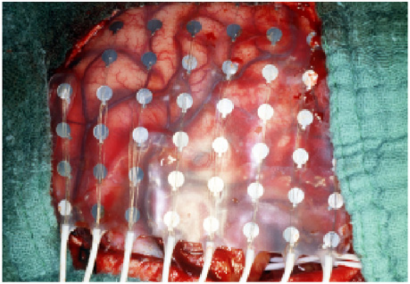

Pistohl et al., 2008 — 10 mm

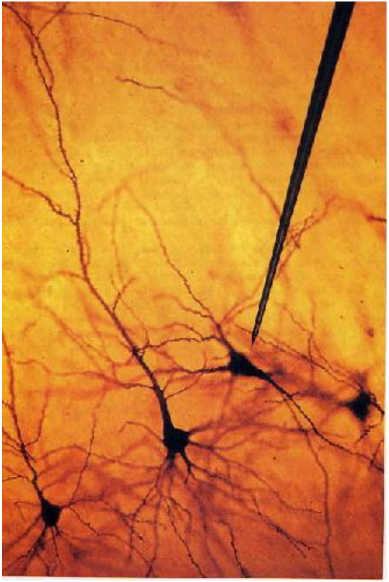

10 μm — Hubel, 1995

Continuous variable systems

Consider a multi-component system, with state variables $y(t)$, driven by fluctuating input $x(t)$. Assume that the system is characterized by a coupling matrix of response kernels $G(t)$ and satisfies the linear consistency equation

$$y(t) = x(t) + (G * y)(t).$$

In the Fourier domain, after taking expectations, we have

$$\langle \hat{y} \rangle = \left[\mathbb{1} - \hat{G}\right]^{-1} \langle \hat{x} \rangle$$

and

$$\langle \hat{y}\hat{y}^* \rangle = \left[\mathbb{1} - \hat{G}\right]^{-1} \langle \hat{x}\hat{x}^* \rangle \left[\mathbb{1} - \hat{G}^*\right]^{-1}.$$

In the case of the Hawkes process, the source term $\langle \hat{x}\hat{x}^* \rangle$ is replaced by $\hat{Y}$. In other words, the spikes of the neurons in the network generate their own "driving noise".

Application to ECoG data

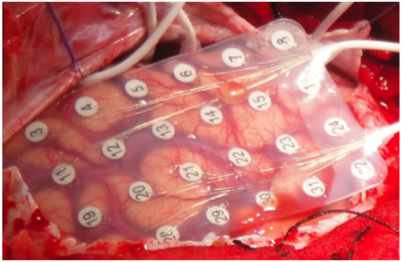

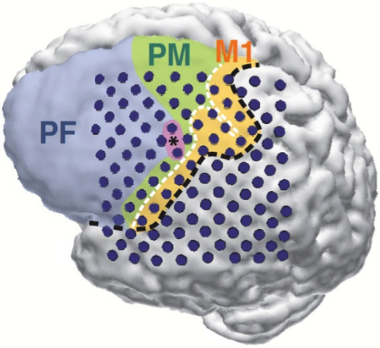

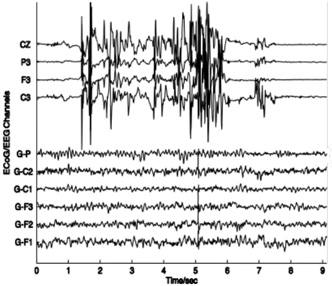

Ball et al., 2009; Derix et al., 2012

Efficient inference of connectivity

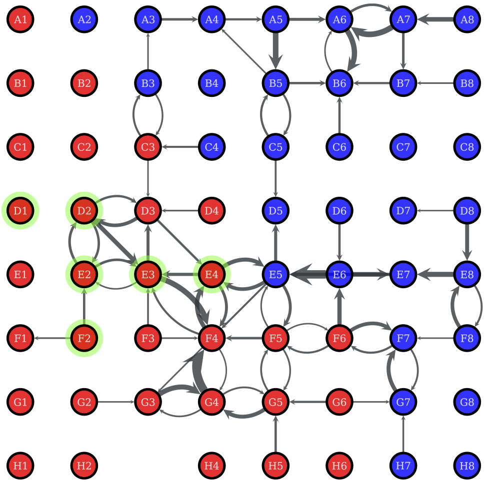

Niederbühl, *Diploma thesis*, 2014

Different frequency channels in ECoG

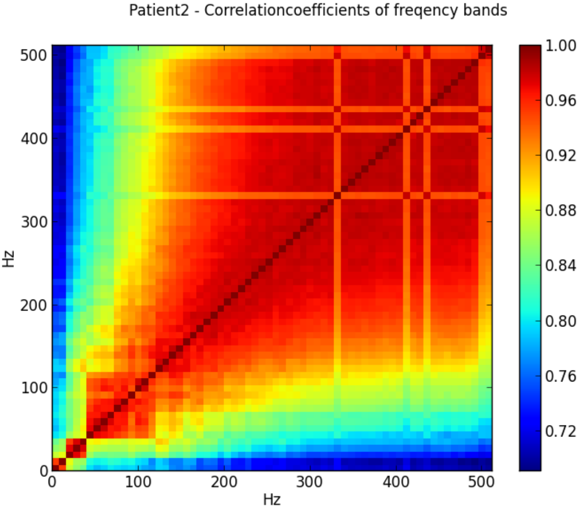

Niederbühl, Schiefer, *work in progress*

Application to MREG data

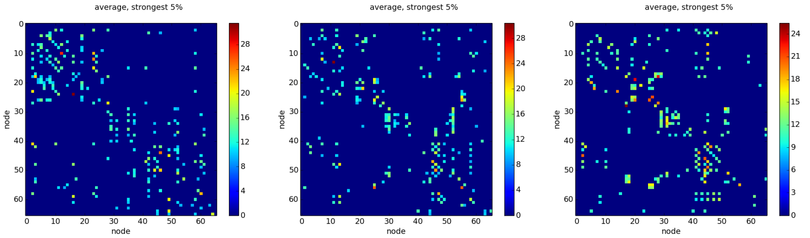

Lee, Zahneisen, Hugger, LeVan, Hennig, *NeuroImage*, 2013
Pernice, Niederbühl, LeVan, *work in progress*

Application to MREG data

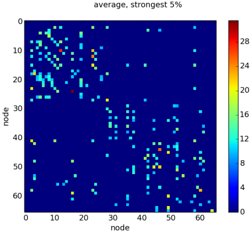

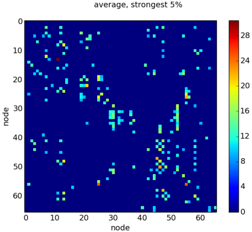

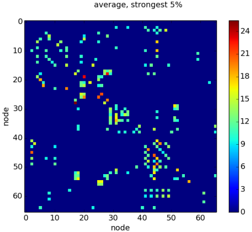

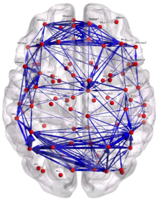

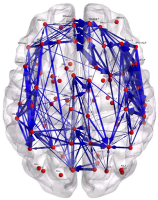

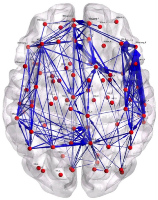

Lee, Zahneisen, Hugger, LeVan, Hennig, *NeuroImage*, 2013
Pernice, Niederbühl, LeVan, *work in progress*

Application to MREG data

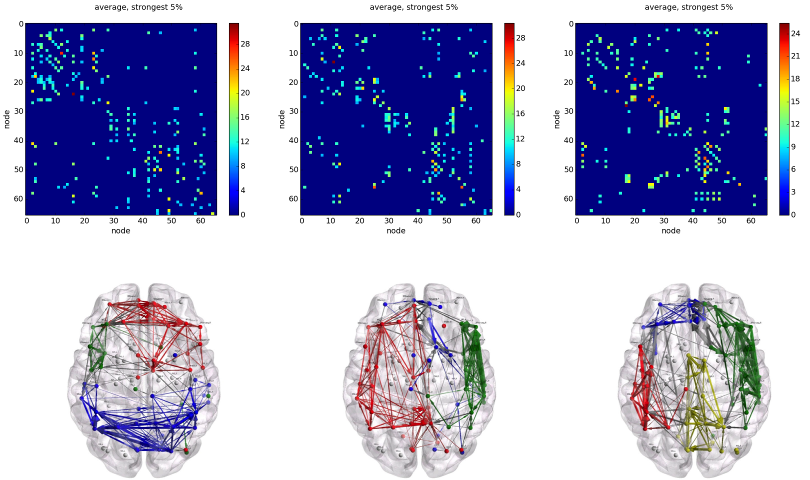

Lee, Zahneisen, Hugger, LeVan, Hennig, *NeuroImage*, 2013
Pernice, Niederbühl, LeVan, *work in progress*

Conclusions

- Linear Hawkes processes are useful models for networks of irregularly spiking neurons. Recurrent networks of LIF neurons can be matched to an equivalent Hawkes process. We expect that this also applies to real nerve cells in neocortical networks.
- Dynamic properties of spiking networks of finite size with arbitrary topology can be inferred analytically, using matrix algebra, provided couplings are weak and spike trains are irregular.
- Pairwise correlations in large networks have strong impact on the amplitude of population signals (LFP, ECoG, EEG, MREG, fMRI). The contribution of specific multi-synaptic pathways (motifs) to pairwise and higher-order correlations can be computed for any given network.
- The micro-topology of sparse networks can be approximately recovered from the covariance matrix, employing compressed sensing methods. Directed links can be inferred from non-directed zero-lag covariances, but accounting for temporal information improves the inference.

Stefano	Cardanobile
Alexander	Niederbühl
Volker	Pernice
Jonathan	Schiefer
John	Hertz
Stojan	Jovanović
Marcel	Sauerbier
Benjamin	Staude
Jürgen	Hennig
Pierre	LeVan
Tonio	Ball
Markus	Kern
Sina	Bert

Thanks!